CrossMark

SEDIMENTS, SEC 1 • SEDIMENT QUALITY AND IMPACT ASSESSMENT • RESEARCH ARTICLE

Urbanization effects on sediment and trace metals distribution in an urban winter pond (Netanya, Israel)

Iris Zohar[1,2] · Nadya Teutsch[2] · Noam Levin[3] · Gail Mackin[4] · Henko de Stigter[5] · Revital Bookman[1]

Abstract

Purpose This paper aims to elucidate urban development-induced processes affecting the sediment and the distribution of contaminating metals in a seasonal pond located in the highly populated Israeli Coastal Plain. The paper demonstrates how an integrated approach, including geochemical, sedimentological, geochronological, mathematical, historical, and geographical analyses, may decipher a complicated and dynamic metal pollution history in a sedimentary environment controlled by anthropogenic activity.

Materials and methods Three short sediment cores were collected from the margins and center of a small urban pond (Dora, Netanya), located within the Israeli Coastal Plain. Profiles of grain size, organic matter (OM), trace metals (Pb, Zn, V, Ni, Cu, Cr and Co), Pb isotopic ratios, and ^{210}Pb activities (center and southern cores) were determined and a geochemical mixing model was employed (southern core). The watershed contour was calculated, and aerial photos and satellite images were examined.

Results and discussion Construction activities in the watershed were chronologically associated with coarse sediment transport and deposition in the margins of the pond. The upper sandy layers were superimposed on layers rich in fine particles and OM, high concentrations of trace metals, and with Pb isotopic composition of more recent petrol. In the ^{210}Pb-dated southern core, deep metal-rich layers with petrol-related Pb isotopic ratios were inconsistent with metal emissions history. These findings point to mobility and migration of recent contamination metals through the coarse upper sediment layers and into deeper denser layers, confirmed also by a geochemical mixing model. Conversely, in the center of the pond, homogeneous fine particles were deposited with metal profiles consistent with regional emissions.

Conclusions A small urban pond was found to provide an important case study for understanding heavy metal pollution records in highly populated regions. The margins of the pond depicted the surrounding urban development and the induced coarse sediment erosion, accompanied with post-depositional metal mobility. Due to the proximate developing residential areas, high metal concentrations accumulated in the margins, overshadowing regional atmospheric pollution levels recorded by sediment at the center of the pond.

✉ Iris Zohar
irisz2910@gmail.com

[1] Dr. Moses Strauss Department of Marine Geosciences, Leon H. Charney School of Marine Sciences, University of Haifa, 31905 Haifa, Israel

[2] Geological Survey of Israel, 95501 Jerusalem, Israel

[3] Department of Geography, Hebrew University of Jerusalem, 91905 Jerusalem, Israel

[4] Department of Mathematics and Statistics, Northern Kentucky University, Highland Heights, KY 41099, USA

[5] Royal Netherlands Institute for Sea Research (NIOZ), 1790 AB Den Burg, Texel, Netherlands

1 Introduction

The abundance of anthropogenic trace metals in atmospheric, aquatic, and terrestrial environments has significantly increased since the onset of the industrial revolution in the mid-nineteenth century. The spread of trace metals was further promoted through construction, industrialization, and, in many cases, by emissions associated with transportation (Nriagu 1996; Pacyna and Pacyna 2001). Lead was significantly introduced to the global environment by leaded petrol combustion, which was replaced by unleaded petrol in the USA and in Europe in the 1970s–1980s (Nriagu 1996) and in Israel in the 1990s (Teutsch et al. 2001). American leaded petrol was used exclusively in Israel until it was replaced by European leaded petrol in 1992. Unleaded European petrol was introduced later on in the early 1990s. The stable isotopic signatures of the American and European petrol-Pb are distinct and, thus, easily distinguished in Israeli sediments and soils and other compartments of the environment (Erel et al. 1997; Teutsch et al. 2001; Harlavan et al. 2010; Zohar et al. 2014; Levy et al. 2015). Other traffic-related trace metals include Zn, V, Cu, Cr, Co, and Ni, although they all may also be emitted from other anthropogenic activities such as industry and construction. Such activities usually accompany the spread of populated areas, mainly urban (Wong et al. 2006), leading to changes in land uses and land covers.

The type of land cover (e.g., rocky or soil coverage) can be of high importance for material transport in natural arid and semi-arid watersheds (Yair and Kossovsky 2002). An extreme case is pure sand coverage (e.g., active sand dune) with nearly complete infiltration of rainwater (Tsoar 1990). Thus, land cover and soil type should be considered when assessing material transport in a watershed. Changes in land cover, from natural to disturbed, are expected to increase sediment and metal recycling and transport, though various metals are impacted differently (Tang et al. 2005). Industrial areas will usually generate greater flux of trace metals than commercial, agricultural, and residential areas (Tiefenthaler et al. 2008). Urbanization rarely occurs homogenously across an entire watershed, resulting in spatial variability of runoff and contribution of contaminating metals (Tang et al. 2005). In arid and semi-arid regions, the geometry of the watershed was found to influence material transport, in both urban (Asaf et al. 2004) and natural sites (Yair and Raz-Yassif 2004). Moreover, urban drainage systems could further affect metal abundance and dispersion due to transport of trace metal-bearing particles.

When reaching the water body, particles may be subjected to secondary transport processes, possibly focusing the depositing material (Blais and Kalff 1995). On the other hand, limited internal transport will allow the sediment to better reflect direct atmospheric deposition of metals originating from a wider region (Weiss et al. 1999; Bookman et al. 2008; Zohar et al. 2014).

Strong sequestration of trace metals is affected by sediment characteristics and is more efficient in fine-grained sediment.

Organic matter (OM) and oxide-hydroxides are strong binding agents (see review by Du Laing et al. 2009), while sandy sediments enable effective mobilization of metals (Balasoiu et al. 2001). Thus, metal accumulation in a sediment core from a populated area could reflect chronological sequestration of metals and/or geomorphologic and geographic processes in the watershed. The anthropogenic fraction of metals in soils and sediments is more accessible to acid leaching than the natural fraction incorporated in aluminosilicates. This enables distinguishing between anthropogenic and natural sources (e.g., Erel et al. 1997; Farkas et al. 2007; Harlavan et al. 2010).

This study describes metal accumulation patterns in a relatively small (ca. 0.055 km^2) winter pond (Fig. 1). Dora Pond is one of the last seasonal ponds to exist along the Israeli Coastal Plain, which has undergone extreme development in the past century (Levin et al. 2009). Although the watershed underwent significant changes in its land cover and use in the past few decades, development activities did not include the pond itself, making it a potential study site for anthropogenic effects on urban aquatic environments. This paper employs a comprehensive approach to decipher urban development-induced changes in deposition of sediment and trace metals, as a case study for pollution records in urban ponds. In a previous study, the contamination sources were identified and the regional metal pollution history was reconstructed based on the homogeneous fine-grained undisturbed profile from the center of the pond (Zohar et al. 2014). Consequently, this core is used here for comparison to the impacted marginal cores.

2 Research methods

2.1 Study area

Dora Pond is located within the city of Netanya, in the heavily built Israeli Coastal Plain (Fig. 1). Yet, the pond does not appear to have changed in recent history, as the line of planted *Eucalyptus* trees along its perimeter is already observed in a 1929 map (Fig. S1, Electronic Supplementary Material). The watershed of Dora winter pond is located between two longitudinal north-south eolionite ridges of ca. 50 m above sea level (masl) (locally known as kurkar ridges; Engelmann et al. 2001). Sand dunes on the southern edge of its watershed reach a height of more than 40 masl, while the base of the pond is about 28 masl. The soils within Dora watershed follow a topographic gradient, starting with sandy clay loam soil on top of the kurkar ridges, gradually changing to higher silt and clay content along the slopes, and ending with a hydromorphic clay (grumusol) soil in the pond itself (Dan 1982). Similar ephemeral winter ponds and marshes were naturally formed along the Israeli Coastal Plain in local troughs with poor drainage (Dan and Yaalon 1990). Since the late nineteenth century, 97% of these wetlands were drained in order to increase land resources and the remaining wetlands
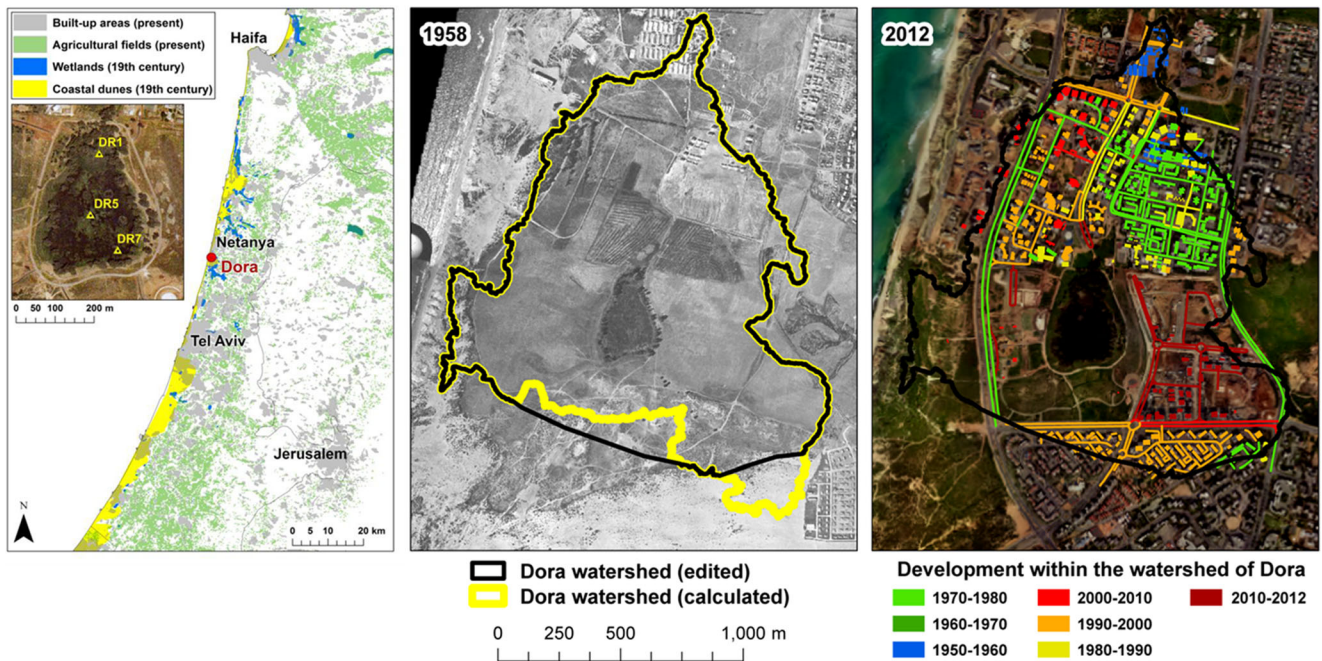
Fig. 1 Left: location map of Dora winter pond, situated in the center of the heavily urbanized Israeli Coastal Plain and a present day close-up aerial photo of Dora Pond, presenting location of sediment cores. *Center*: Dora Pond's watershed boundaries before major building construction took place. *Right*: development of built-up areas (buildings and paved roads) within the watershed of Dora Pond (same scale as center photo)

became highly affected by agriculture, urbanization, and industrial development (Levin et al. 2009).

2.2 Geographical analysis

The watershed of Dora Pond was calculated using detailed contours (at a vertical interval of 0.5 m) shown on 1:500 maps (based on a photogrammetric survey from 2005) obtained from the Municipality of Netanya. A digital elevation model from these contours was created at a spatial resolution of 1 m using the INTERCON interpolation method available in IDRISI Selva GIS (Clark 2012). The first step for calculating the watershed was filling local sinkholes in the DEM using ArcGIS Spatial Analyst. The horizontal accuracy of the derived watershed is estimated to be in the order of about 250 m. The resulting calculated watershed penetrated southeast, into areas of former active sand dunes. Originally, all rainfall would infiltrate in the active sand dunes and would not contribute to the pond. At a later stage (since the 1970s), this area was impacted by topography changes associated with construction of residential areas to the south of Dora Pond and the consequent land flattening. The editing was performed to reconstruct the watershed as it had been before the urban development as realistically as possible.

2.3 Sediment sampling, processing, and analysis

Three sediment cores were retrieved from Dora Pond in 2011: DR1 (23 cm) from the northern margin, DR5 (40.5 cm), from the center, and DR7 (23 cm) from the southern margin (Fig. 1). Sampling was done by pushing a 54-mm diameter PVC tube into the ground during the dry period in order to avoid compaction. One-centimeter sediment slabs were cut in the field (0.5 cm slabs at the top 2 cm of DR1) then kept cool until reaching the laboratory where they were frozen. The samples were freeze dried, and the coarse particulate OM (CPOM, e.g., roots and branches) was removed. All marginal samples (25 and 23 in DR1 and DR7 cores, respectively) were analyzed. In DR5 core (21 samples), high-resolution analysis was conducted in the upper part, focusing on changes in the modern era, while lower resolution analysis was performed in the lower part, which indicated constant trends (e.g., Erel et al. 1997; Townsend and Seen 2012). Particle size distribution was determined on triplicate sub-samples by a laser diffraction grain size analyzer (Beckman Coulter) after H_2O_2 treatment (standard deviation <5%). Dry bulk density was calculated, taking into account the specific mass of mineral and OM and the presence of air in the interstitial space. The fine OM content of the sediment was determined by a "loss-on-ignition" (LOI) procedure (incinerating in 550 °C for 4 h, without decomposing carbonates; Dean 1974) on duplicate sub-samples (repetition better than 5%).

Total (supported and excess) ^{210}Pb activity was measured by alpha spectrometry via the ^{210}Pb granddaughter isotope ^{210}Po (counting error <3%; see De Stigter et al. 2011 for ^{210}Pb methodology details). This dating method is applicable for the past ~150 years (^{210}Pb half-life of 22.3 years), where excess ^{210}Pb activity is detected (upper 12 cm in core DR5 and

19 cm in core DR7). The constant rate of supply model, which assumes a constant flux of ^{210}Pb but variable mass accumulation rate (Appleby and Oldfield 1978), was used to calculate sediment accumulation rates and ages. The density of the major constituents in each profile (DR5: clay and DR7: sand in the upper section and clay and OM in the lower section) was applied in these calculations.

For the labile fraction of trace metals, duplicate sub-samples were leached using a dilute acid solution (0.5 M HNO_3, Erel et al. 1997; hereafter named "leach"). Whole sediment concentrations of trace elements (hereafter named "total") were determined in duplicate samples following dissolution by acid mixture (digestion on a hot plate with HNO_3, HF, and HCl). Trace metal (Pb, Zn, V, Ni, Cu, Cr, and Co) concentrations were determined by ICP-MS (Perkin-Elmer). Differences between duplicate sub-samples were lower than 5% (excluding 4% of the duplicates with 6–11%, 4% with 10–30%, and 0.5% with >50% difference) for the leach and lower than 7% (excluding 10% of the duplicates with 8–20% difference) for the total concentrations. Standards yielded 2.6% precision and 4.3% accuracy. Isotopic composition of the leach Pb was measured after column separation of Pb (Ehrlich et al. 2004) by MC-ICP-MS (Ehrlich et al. 2001; Platzner et al. 2001) (Nu Instruments), along with repeated measurements of the SRM 981 standard for accuracy and precision control (Platzner et al. 2001). Further analytical details can be found from Zohar et al. (2014).

A geochemical mixing model was used to determine relative contributions of Pb from various sources in the complex DR7 sediment profile, based on their isotopic ratios. Model description, results, and sensitivity analysis are presented in the Supplementary Information.

3 Results

3.1 Urbanization in the watershed—geographical analysis

The calculated and edited watershed contours were superimposed on historical maps, aerial photos, and satellite images of the region, over the course of its development from the late nineteenth century till recent years (Fig. S1, Electronic Supplementary Material). A summary (by decade) of the development of the watershed is shown in Fig. 1. The calculated watershed seems to roughly correspond to the geomorphological limits set upon it by the sand dunes to the south and the coastal cliffs to the west as well as to the distribution of past local winter ponds (each indicating a local watershed; see the 1943 map, Fig. S1, Electronic Supplementary Material). Due to the coarse-grained texture of sand, active dunes with no vegetation cover have low moisture content at field capacity and rainwater percolates easily into the sand (Tsoar 1990). Biological crusts, which were shown to generate runoff on

dunes (Yair 1990), are quite uncommon along the Israeli coastal dunes (Levin et al. 2007). Therefore, sand inputs are not expected to have reached the pond from the southern direction before the human-made topographical changes. Prior to the founding of the city of Netanya in 1929 (Fig. S1, Electronic Supplementary Material, and Fig. 1), there were no villages nor towns in the area, which was sparsely inhabited by Bedouins. The first buildings within the Dora watershed were built to the north of the pond in the 1950s. The neighborhood of "Ne'ot Shaked" was well established by 1975. The development of "Kiryat Nordau" neighborhood, to the southeast of Dora Pond, was mostly restricted to the active sand dunes area. However, some parts of it were within the Dora watershed and could thus impact the runoff into the pond, as construction progressed northwards in the 1970s. The 1989 false color Landsat composite (Fig. S1, Electronic Supplementary Material) reveals that the clearing of vegetation and exposure of sandy soil took place in the southern part of the Dora watershed in the late 1980s (seen as a bright area in this Landsat image), preceding the building of the "Giv'at Ha'Irusim" neighborhood. A recreational park was developed around the pond and to the west in the late 2000s. In recent years, the new neighborhood "Agamim" was built just to the east of Dora Pond, within the watershed boundaries (Fig. 1 and Fig. S1, Electronic Supplementary Material).

3.2 Lead-210 activity profiles

Lead-210 dating was performed on the DR5 and DR7 cores (Table S1, Electronic Supplementary Material). In the DR1 core, background concentration levels were not reached, suggesting that the bottom layers are relatively recent and that the supported ^{210}Pb cannot be evaluated, making ^{210}Pb dating impossible. In the DR7 core, the maximum observed activity was 99.7 mBq g^{-1} (depth 1–2 cm) and the supported value (21.0 ± 2.4 mBq g^{-1}) was determined based on the bottom 4 cm (19–23 cm). The top 19 cm were dated from present down to the mid-nineteenth century, and the deepest sediment was roughly estimated to represent the late eighteenth century. Although a general decreasing trend prevailed, the excess ^{210}Pb activity in the DR7 profile was irregular, with three zones of local maximum (Fig. 2): at 1–3, 7–10, and 15–19 cm (peaking at 16.5 cm). The DR5 core displayed a regular exponential activity profile, with maximum and supported ^{210}Pb activities of 165.2 and 30.4 ± 2.9 mBq g^{-1}, respectively (Zohar et al. 2014), which are higher than in the DR7 core (Fig. 2 and Table S1, Electronic Supplementary Material). The sediment accumulation rate in both dated cores was lowest (0.03 g cm^{-2} $year^{-1}$) in the late nineteenth century. The maximum rate was recorded in the southern margin (DR7) during the early 1990s (0.63 g cm^{-2} $year^{-1}$ at a depth of 6.5 cm), about sixfold higher than in the center, DR5 core (0.11 g cm^{-2} $year^{-1}$ at depth of 4.5 cm), recorded in the
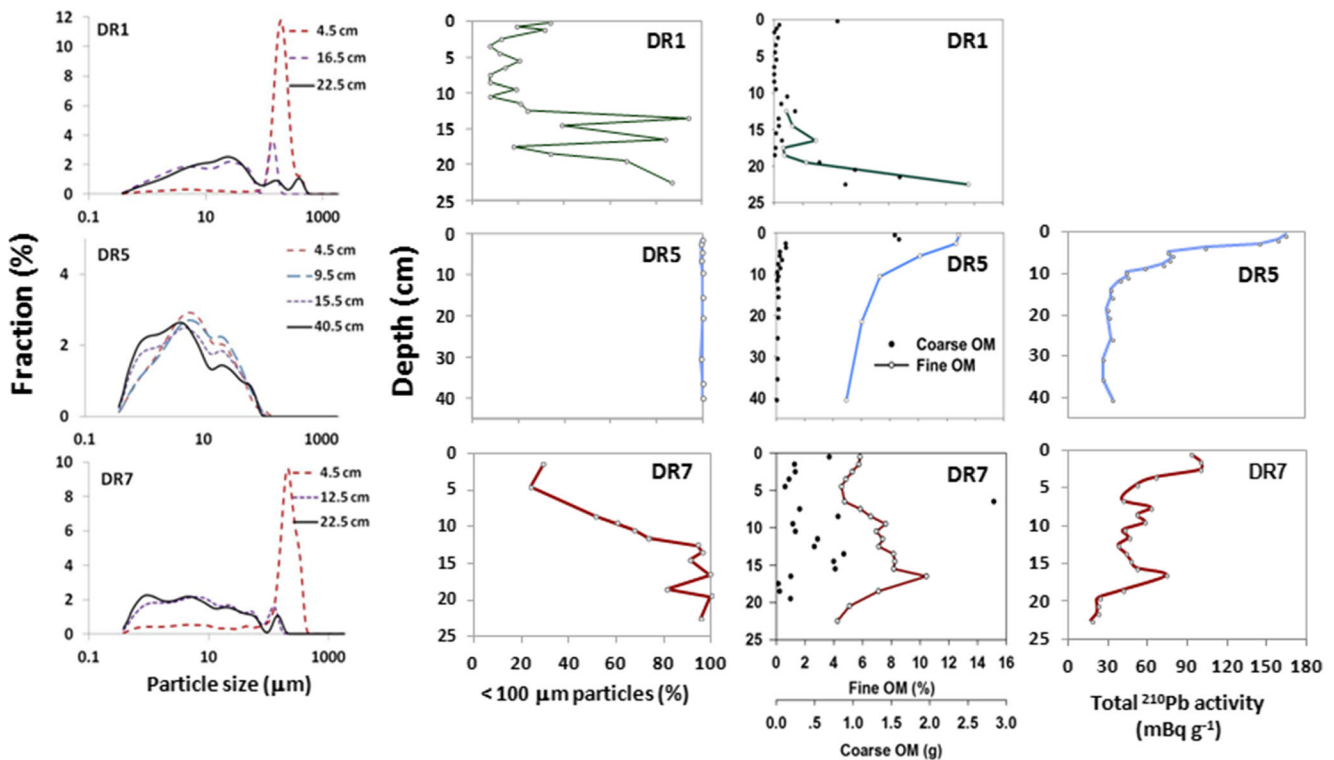
Fig. 2 Sedimentary features in cores from the northern margin (DR1), center (DR5), and southern margin (DR7) of Dora Pond, including particle size distribution in selected depths and profiles of the <100-µm-sized particles, fine and coarse organic matter (OM), and total ²¹⁰Pb activity. *Lines* between measured values are interpolation

1970s (Fig. 3 and Table S1, Electronic Supplementary Material). This strong timing divergence implies different impacting sources.

3.3 Texture and organic matter distribution

Sediment from the northern and southern margins of the pond (cores DR1 and DR7, respectively) consisted of two particle size populations, splitting around 100 µm. The DR1 core exhibited sequences of sand interlaid by fine particles at the top 19 cm while in the DR7 core, the >100 µm particles predominated in the top 8 cm and gradually decreased from 9 to 12 cm. In both cores, the fine fraction prevailed until the bottom. The maximum content of particles >100 µm was 92% and 76 in DR1 (7–10 cm) and in DR7 (4.5 cm), respectively (Fig. 2). This sediment characteristic is in strong contrast to the center of the pond (DR5) where the sediment consisted almost exclusively of particles <100 µm (0 to 0.8% of particles >100 µm in DR5, Fig. 2). The <100 µm fraction common to the three cores, included distinct modes at 1, 5, 20, and 50 µm (Fig. 2) and was of mineral and organic composition. The mineralogy of the fine sediment from the center of the pond (DR5) was governed by clay minerals (specifically, montmorillonite; Koyumdjisky et al. 1988; Zohar et al. 2014). In the northern margin core (DR1), the >100 µm fraction included a distinct mode around 185 µm

throughout most of the core, and at 147 and 373 µm, in the bottom 4 cm. At the southern margin core (DR7), distinct modes in the >100 µm fraction were at 213 (upper profile) and 147 µm (mid till bottom profile, Fig. 2).

Elevated levels of fine OM content and buried CPOM were abundant in deeper layers of the DR1 (19–23 cm) and DR7 (8–16 cm) cores (Fig. 2). Among the buried CPOM, some residues of plants very common to the pond were well preserved and easily recognized, like *Eucalyptus* seeds in the DR1 core and *Butomus umbellatus* roots in the DR7 core. The sediment from the center of the pond (DR5) displayed an orderly degradation profile of OM, indicating undisturbed down-profile decomposition (Fig. 2).

To summarize, the marginal sediments from the pond were heterogeneous and included deep layers associated with fine particles and OM, superimposed by younger sandy layers.

3.4 Trace metal concentrations

Leach trace metal concentrations are shown in Fig. 4 and Table S2 (Electronic Supplementary Material). High concentrations of trace metals were found in deep layers of the marginal cores. In the northern DR1 core, leach trace metal concentrations fluctuated concomitantly throughout the depth profile with a substantial increase in the lowermost 4 cm of the core (Fig. 4) and an exceptionally high Zn concentration
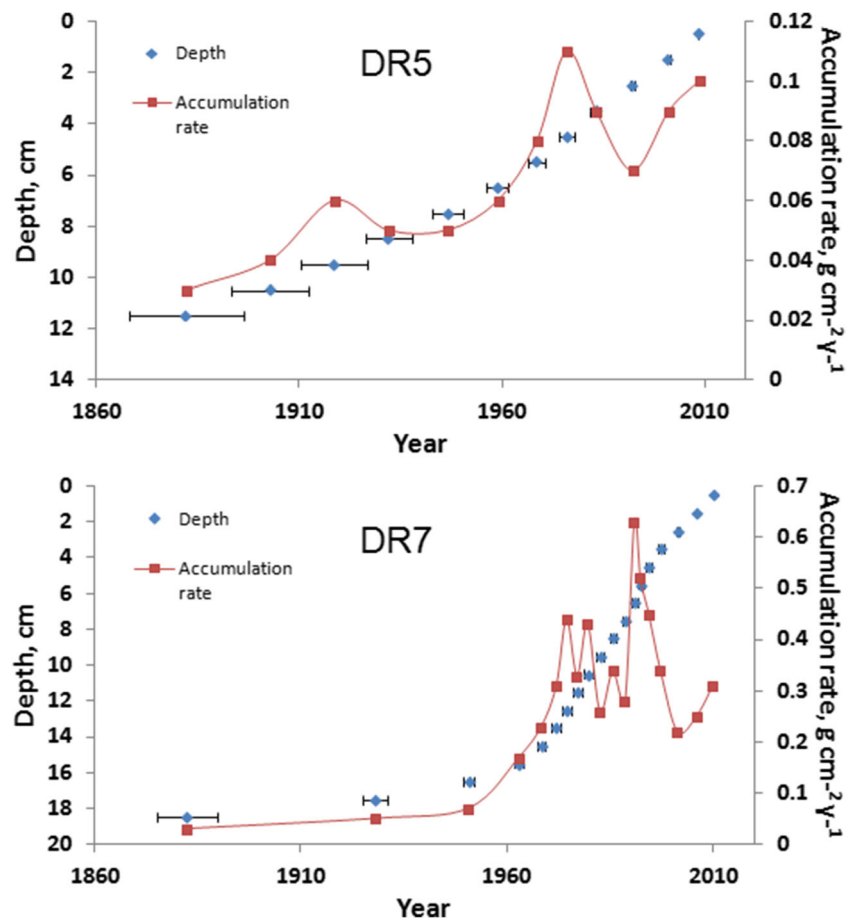
(1100 µg g^{-1} at depth of 21.5 cm). In the southern DR7 core, elevated levels of all studied trace metals were obtained at the depth range 9–19 cm. Maximum metal concentrations were considerably higher in the marginal cores compared to the center DR5 core, where trace metal concentrations usually peaked in the upper few centimeters, after starting to increase above background levels only from a depth of 12 cm (Fig. 4). For example, maximum leach Pb concentration in DR7 was 59.1 µg g^{-1}, at depth of 14.5 cm, about twice that of DR5 (30.9 µg g^{-1} at depth of 2.5 cm). Total metal concentrations

followed the leach concentration trends in all three profiles (Table S2, Electronic Supplementary Material).

3.5 Lead isotopic composition

The ^{206}Pb/^{207}Pb profiles of leach Pb obtained from the three locations in the pond exhibit different trends (Fig. 5). Both the DR1 and DR7 profiles contained low ^{206}Pb/^{207}Pb values in deep layers (e.g., 1.14–1.17, Fig. 5). These values were inconsistent with the chronological trend, indicated by the center
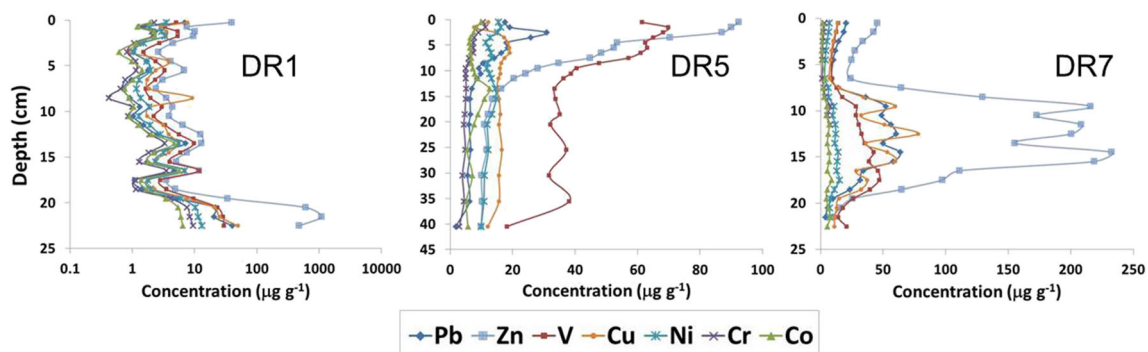
Fig. 4 Depth profiles of trace metal leach concentrations in the northern margin (DR1; logarithmic scale), center (DR5), and southern margin (DR7) of Dora Pond. *Lines* between measured values in DR5 are interpolation

Fig. 5 Depth profiles of leach Pb stable isotopes ratio (^{206}Pb/^{207}Pb) from the northern margin (DR1), the center (DR5), and the southern margin (DR7) of Dora Pond
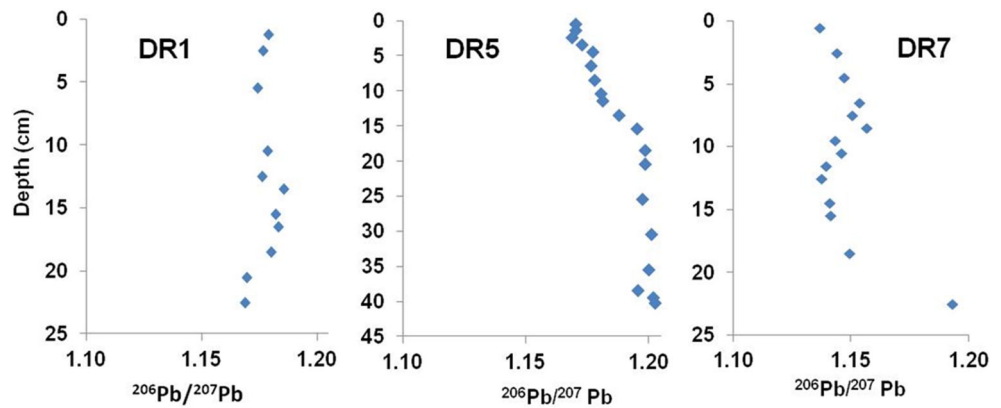

DR5 profile, which displayed a shift from natural Pb isotopic ratio (ca. 1.20) in the lower part of the core, towards lower values indicative of anthropogenic Pb (ca. 1.17) in the upper part (Zohar et al. 2014).

Isotopic ratios of leach Pb (^{206}Pb/^{207}Pb and ^{208}Pb/^{206}Pb) from Dora sediment were compared to potential Pb sources in order to elucidate the major contributors to the Pb inventory in the pond. The potential sources include uncontaminated Israeli soils (Erel et al. 1997; Teutsch et al. 2001), Saharan dust (Erel et al. 2006), aerosols from Cairo and Eastern Europe (Erel et al. 2006, 2007), and the petrol used in Israel: pre-1992 (American) petrol and post-1992 (European) leaded and unleaded petrol (Erel et al. 1997). A detailed description of the Pb potential sources can be found in Table S3 (Electronic Supplementary Material) and in Zohar et al. (2014). It should be noted that current unleaded European petrol (measured recently in our laboratory) contains negligible levels of Pb (<5 μg L^{-1}). Thus, inputs from this source should be attributed mostly to the late

1990s, when isotopic analysis of the unleaded European petrol was attained (Erel et al. 1997).

On a plot of ^{208}Pb/^{206}Pb vs. ^{206}Pb/^{207}Pb, samples from Dora Pond fell within the Pb isotopic compositions of natural and petrol-Pb potential sources (Fig. 6). Only the deepest sample in DR7 was on the natural sources line, while all other samples were aligned on the upper part of the petrol-Pb line, nearest to the post-1992 petrol-Pb value. The DR7 samples from the depth range 10.5–18.5 cm displayed a significant contribution of the post-1992 European end-members, more than in upper sediment samples. Similarly, Pb isotopic composition values in DR1 were not chronologically aligned on the petrol-Pb sources line, with the lowermost sample displaying values typically associated with anthropogenic influence (e.g., ^{206}Pb/^{207}Pb of 1.17 at depth of 22.5 cm, Figs. 5 and 6). DR5 Pb isotopic composition values were chronologically aligned: lower profile samples were on the natural sources line while upper part samples were on the petrol-Pb sources line.

Fig. 6 Lead stable isotope ratios (^{208}Pb/^{206}Pb vs. ^{206}Pb/^{207}Pb) in samples from the northern margin (DR1), center (DR5), and southern margin (DR7) of Dora Pond, together with isotopic signatures of potential Pb sources. *1* Erel et al. (1997), *2* Teutsch et al. (2001), *3* Erel et al. (2006), *4* Erel et al. (2007), *5* Díaz-Somoano et al. (2009); see Zohar et al. (2014) for details
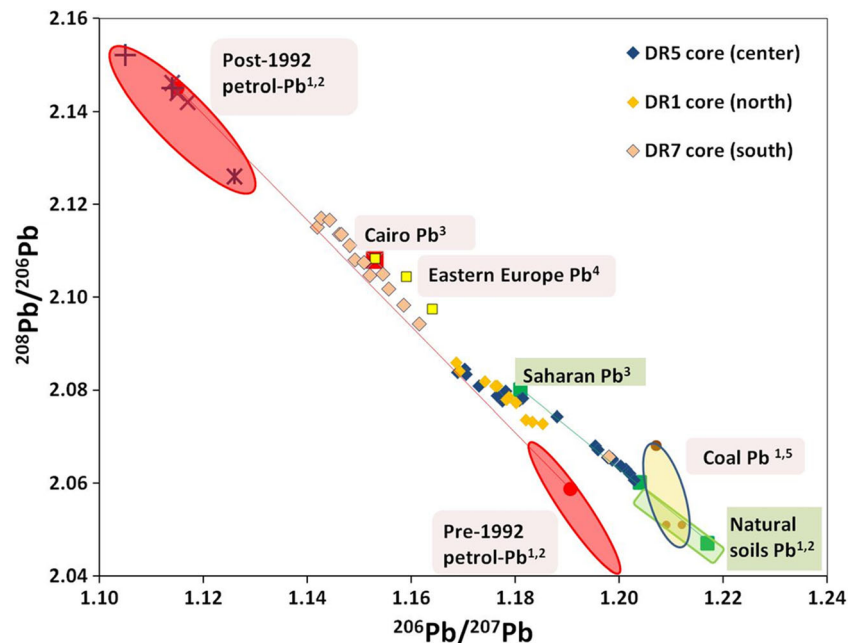
4 Discussion

4.1 Sedimentation effect on ^{210}Pb activity

Different inventories of excess ^{210}Pb activity were found in the center (DR5) and in the southern margin (DR7) of the small pond (Fig. 2). Variability in ^{210}Pb inventory among sites within the same watershed can result from differences in mineralogy, grain size, organic content, and accumulation history of the ^{210}Pb carrying particles (e.g., Guevara et al. 2003). The sediment profiles in the two locations indeed differ in their physical features. The uniform dominance of the particles <100 μm and the ^{210}Pb decay trend in the DR5 center core reflects a quiescence depositional environment. This resulted in the formation of a regular exponential decay trend and a dated metal profile, which could be well correlated with regional historical records (Zohar et al. 2014).

In the heterogeneous southern margin sediment DR7 profile, excess ^{210}Pb generally decayed within the upper 19 cm, representing ca. 150 years (Fig. 2). However, in these layers where the excess ^{210}Pb activity was expected to wane due to time-dependent decay, the ^{210}Pb profile implied leaching down of ^{210}Pb into sediment constituents which served as a sink. The irregularity of the ^{210}Pb activity profile appears to be impacted by discontinuous sedimentation processes, including the size and nature of the accumulating particles (e.g., He and Walling 1996). Normally, higher ^{210}Pb levels would be associated with fine-grained sediment (of relatively high particle surface area) and lower levels of ^{210}Pb activity with sandy layers (of relatively low particle surface area). However, the excess ^{210}Pb activity correlation with the fine texture (specifically, the <100 μm fraction) in the southern DR7 core was especially low in the whole profile ($r^2 = 0.05$) as well as at the fine particle-rich depth range (9–23 cm; $r^2 = 0.15$). On the other hand, the excess ^{210}Pb activity had a high correlation ($r^2 = 0.89$; Fig. 7) with the fine OM in the lower part of the profile (9–23 cm) but exhibited a low correlation with fine OM both in the whole profile and in the upper sandy part ($r^2 = 0.002$ and 0.07 (Fig. 7), respectively); this is because the ^{210}Pb influx is continuous, while OM accumulation could have been impacted by changes in the sedimentary environment. Similarly, a high correlation ($r = 0.90$) between ^{210}Pb flux and OM content was also found by Guevara et al. (2003) in upper sediment layers of three lakes. Positive correlation between OM content and metal concentration levels within a sediment profile can evolve from leaching down of dissolved organic carbon (DOC), formed during degradation of buried OM, which may mobilize fine particles or metal complexes (e.g., Richards et al. 1998; Biester et al. 2012; and references therein). A similar impact of sedimentary features on displacement of isotopic time tracers was reported by Ciszewski et al. (2008). In order to support the radiometric dating, it should be complemented with available non-radiogenic time markers, such as historical records (Kirchner 2011). Indeed, Ciszewski et al. (2008) resolved the
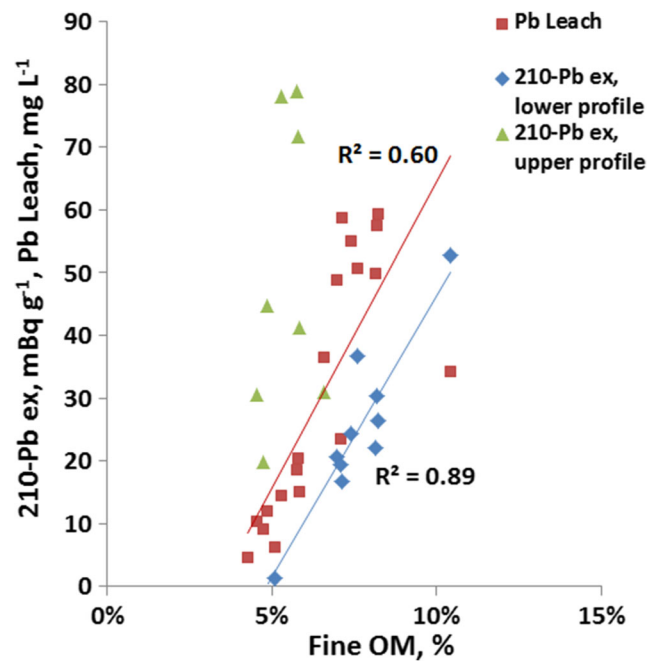

Fig. 7 Lead vs. fine OM content in DR7 core. *Upper profile*: 0–8 cm (with poor correlation, $r^2 = 0.07$). *Lower profile*: 9–23 cm

uncertainty by comparing their radiometric dating results to the local history of river pollution and sediment deposition. Thus, in this research, geographical, sedimentary, and geochemical evidence of known chronology was further compared and related to the potentially tentative dating of the southern DR7 core (Table S1, Electronic Supplementary Material).

4.2 Urbanization effects on sedimentation

Sediments that accumulated in the margins of Dora Pond recorded urbanization effects in the watershed and its surroundings. Thus, the marginal sediments may provide a unique case for examining effects of urban anthropogenic processes on natural sedimentary environments. Construction activities around the pond enhanced surface erosion of the local destabilized sand dunes or contributed extrinsic sand which was employed in the construction sites, resulting in significant amounts of sand transported to the pond's margins. The insignificant amounts of sand in the center of the pond (DR5) indicate negligible transport of coarse grains from the ponds margins, eliminating the possibility of sediment focusing towards the center, in agreement with the relatively plain nature of the pond's bottom (Koyumdjisky et al. 1988). The significant sand inputs in the margins were reflected in high accumulation rates compared to the center of the pond (DR5). In the DR7 southern margin, the maximum accumulation rate attained in the upper sandy layer was dated to the early 1990s, when the nearest neighborhood to the south of the pond (Giv'at Ha'Irusim) was constructed (Fig. 1 and Fig. S1, Electronic Supplementary Material). In the center (DR5), the

maximum accumulation rate, attained in the 1970s, was significantly lower. Moreover, the first appearance of sand in the southern margin was dated to the mid-1970s (Table S1, Electronic Supplementary Material), when construction activity took place at the southernmost tip of the watershed (Kiryat Nordau neighborhood, Fig. 1 and Fig. S1, Electronic Supplementary Material). This implies the feasible impact of relatively distant sand dunes in the watershed due to disturbances by construction, resulting in runoff and material transport to the pond. Sand delivery to the southern margin of the pond continued thereafter, as indicated by the continuous sandy upper DR7 profile.

It follows that the sandy layers predominating depth of 19 cm, and upwards in DR1 northern core, originated from construction activity in the northern part of the watershed. The building of the Ne'ot Shaked neighborhood, starting in the late 1950s and continuing until the late 2000s, is probably the cause of the continuous input of sand to the north of the pond (Fig. 1 and Fig. S1, Electronic Supplementary Material).

The OM features in the marginal profiles also appear to be affected by the urbanization in the watershed. Both profiles include buried fine and coarse OM below sand layers that has been shown to correlate with the neighborhoods' development within the watershed. A combination of urbanization and sedimentation effects could result in longer dry seasons in the pond's margins, leading to retardation in OM decomposition. For example, the installation of drainage systems in the residential areas would result in smaller amounts of water arriving to the pond, primarily affecting the marginal perimeter. Additionally, the low water holding capacity of sand (Richards et al. 2000) results in extensive loss of water from sandy profiles.

4.3 Sedimentation effects on metal distribution

Apparently, the accumulation of the marginal sediments was affected by urbanization in the watershed, which in turn impacted the metals' unusual depth distribution. Both marginal cores displayed non-chronological patterns of metal profiles. High levels of trace metals and post-1992 European petrol-Pb isotopic signature were concentrated in deep layers of fine particles and substantial CPOM, while the younger, sandy layers above attained isotopic traces of pre-1992 American leaded petrol. This unique pattern is in contrast to the consistent pollution record found in the center of the pond, DR5 core (Zohar et al. 2014). Typically, concentration increases from background levels in historical pollution records (Heim and Schwarzbauer 2013) are attributed to the human activity since the beginning of the industrial revolution (e.g., Bookman et al. 2008; Vane et al. 2011). Specifically, the marginal metal leach concentration profiles were inconsistent with the regional history of metal emissions (Zohar et al. 2014). The only parts consistent with chronology are the topmost anthropogenic sediments and the lowermost natural layer. In the upper few centimeters, the relatively low Pb concentrations and the low

$^{206}Pb/^{207}Pb$ ratio values indicate that Pb is probably predominated by post-1992 unleaded European petrol (mostly attributed to the late 1990s exposure), also confirmed by the mixing model analysis (Fig. S2, Electronic Supplementary Material). This is consistent with the use of unleaded petrol in recent decades (Teutsch et al. 2001; Zohar et al. 2014). The deepest sediment (22.5 cm) is older than the mid-nineteenth century (Table S1, Electronic Supplementary Material) and consistently attained low trace metal concentrations and a Pb isotopic signature of natural sources (Fig. 6). Restricting the geochemical end-members in the mixing model at the bottom layer to only natural sources reveals the natural soil proportion was approximately 75% (similar to the overall run, Fig. S2, Electronic Supplementary Material) and the remaining 25% due to Saharan dust. These proportions may have interesting significance for understanding pedogenetic processes, potentially elucidating the Saharan dust contribution to the formation of clay soils in the Coastal Plain of Israel (Yaalon and Ganor 1973; Gvirtzman and Wieder 2001).

Above the bottom layers of the southern DR7 core, an abrupt increase in the trace metal levels and a decrease in Pb isotopic compositions were recorded in the layers dated between 1960 to mid-1980s. Both the $^{208}Pb/^{206}Pb$ vs. $^{206}Pb/^{207}Pb$ data (Fig. 6) and the mixing model results (Fig. S2, Electronic Supplementary Material) indicate a significant contribution of the post-1992 European end-member in this metal elevated section. Moreover, the sensitivity analysis of the mixing model for this depth range indicates that European petrol-Pb was the predominating end-member in all cases of tested variability. Yet, until 1992, only American petrol-Pb was in use in Israel. The sediment section previously dated to ca. 1985 to 1992, encompasses the period of maximum (American) petrol-Pb emissions in Israel, peaking in 1988 (Teutsch 1999; Zohar et al. 2014), consistent with the Pb isotopic ratio signature (Fig. 6 and Fig. S2, Electronic Supplementary Material). However, Pb concentrations in this sediment section were lower than in the metal enriched section below it. Although not dated, the northern core (DR1) exhibited similar trends as the southern core (DR7). In the upper part of the profile, metal concentrations were relatively low and sequences of natural and petrol sources governed Pb isotopic composition. Yet, in the deeper profile, fine particles and high content of CPOM were associated with significantly elevated metal concentrations and strong isotopic signature of European petrol-Pb.

The peculiar metal concentration profiles and the non-chronological distribution of Pb isotopic composition point to post-depositional metal mobilization in the margins of the pond. Trace metals seem to leach downwards through the sandy upper layers into the deeper fine particles and organic-rich layers, where they were more strongly sequestered. Similarly, Ciszewski et al. (2008) reported downward migration of polluting metals through heterogenic sediment profiles, to pre-industrial

fine-grained layers. Likewise, trace metal mobility observed in river sediments was attributed to sediment type and mineralogy (Slowik et al. 2010; Gonzalez-Fernandez et al. 2011). Indeed, significant correlations between cation exchange capacity, clay or OM content, and metal content in floodplains, soils, and wetlands are often reported (see review by Du Laing et al. 2009). Conversely, sandy soils are less prone to retain metals (Rieuwert et al. 1998 and references therein; Balasoiu et al. 2001). Hence, higher metal mobility is expected with an increase of the sandy fraction. In the southern DR7 core, trace metal content decreased concurrently as the fraction of the >100 μm increased in the sediment profile from 13 to 6 cm. Interestingly, the major concentration change occurred where the coarse fraction content fell below 50% (depth 8.5 to 7.5 cm), similar to that of Balasoiu et al. (2001). Organic matter content in soils may play a major role in metal retention (Balasoiu et al. 2001). The increased fine and coarse OM content in deeper layers has probably contributed to sequestering leaching metals from upper sandy layers. However, the presence of coarse roots and seeds may impose light packing of the hosting sediment, contributing to further metal migration by trickling down of fine particles and leaching DOC (Temminghoff et al. 1997; Richards et al. 1998; Biester et al. 2012) as was suggested above for ^{210}Pb. Also in the southern DR7 core, the correlation of leach Pb concentrations and fine OM is 0.60 for the whole profile (Fig. 7), while the correlation with fine particles was similar ($r^2 = 0.55$) only in a limited depth range (8.5–14.5 cm). These results are consistent with the high correlations of fine OM and ^{210}Pb in the lower part of the profile (Fig. 7), emphasizing the greater role of OM in governing Pb redistribution (and likewise other trace metals) in the southern marginal DR7 profile of the pond. An exception is at depth of 16.5 cm where the maximum fine OM (10.4%) was strongly correlated with ^{210}Pb but less so with leach Pb (see also Fig. 2). While ^{210}Pb is geogenic, the stable Pb isotopes originate mostly in the petrol air pollution. Thus, different sources may result in different fluxes and different distribution in the sediment profile. In the upper sand-dominated 12 cm of the northern margin (DR1), the fine OM content was not detectable and leach Pb concentrations had an r^2 correlation of 0.58 with the fine particles. Below 12 cm, where fine particles and OM content grew significantly, leach Pb concentrations were correlated with both parameters (r^2 about 0.87).

The profiles of the various trace metals in the margins usually presented similar trends, including highly mobile Zn and relatively immobile Pb (Martin and Coughtrey 1982; Han et al. 2003; Fonseca et al. 2011). Only limited impact is attributed here to different percolation rates, which could evolve from a different response of each metal to the soil features such as texture (Du Laing et al. 2009), OM content, pH, and competition by other metals (Fonseca et al. 2011). While displaying a similar trend as the other trace metals, Zn concentrations in the deep layers were exceptionally high. This is attributed to high atmospheric fluxes of Zn in recent decades

(Rauch and Pacyna 2009), as found for the center of Dora Pond, DR5 core (Zohar et al. 2014).

Lead migration velocity through the DR7 profile may be roughly assessed by a compilation of various data. Layer of 4–5 cm was dated to 1993–1996, just after the first introduction of the leaded European petrol-Pb which is easily distinguished from the American petrol-Pb (Erel et al. 1997; Teutsch et al. 2001). Results from the mixing model indicate that by the time of sampling in 2011, the leaded European petrol-Pb had penetrated to a depth of 19 cm. That yields a maximal migration velocity of ca. 0.78 cm year^{-1}. Similarly, values up to 0.7 cm year^{-1} were obtained for Israeli soils in other studies (Erel et al. 1997; Teutsch 1999; Teutsch et al. 2001). American petrol-Pb displayed less displacement, possibly since it was already occluded in small clay aggregates upon deposition or prior to it. Yet, even with minor migration, the signature of the regionally substantial emissions of the American petrol-Pb in the late 1980s was not observed in the southern sediment (DR7) as it was in the center of the pond (DR5), since it was probably overshadowed by the later inputs of migrating European petrol-Pb. In the late 1980s–early 1990s, construction and urbanization edged closest to the southern margin of the pond (Fig. 1 and Fig. S1, Electronic Supplementary Material), concurrent with the first introduction of European petrol-Pb in Israel. Similarly, the populated area to the north of the watershed doubled since the 1990s (Fig. 1 and Fig. S1, Electronic Supplementary Material), limiting the signature of the vast American petrol-Pb emissions in the late 1980s in the receiving deep layers in the northern margin sediment (DR1). The high proximity of residential areas and traffic passage could result in substantial Pb fluxes within soils and sediments, higher than background values of regional atmospheric pollution (Walraven et al. 2014). Thus, the local and very proximate inputs of the European petrol-Pb overwhelmed the regional 1980s' inputs in the margins of Dora Pond.

The heterogeneous composition of the sediment from the margins of Dora Pond enables continuous post-depositional mobilization of trace metals, mostly in the wet season, resulting in a dynamic metal status in the profiles.

5 Conclusions

Sediment cores from the Dora Pond located in the populated Israeli Coastal Plain demonstrate effects of urban development on aquatic environments. This relict pond recorded the urban development in its watershed as construction-related erosion enhanced sand transport to the margins of the pond, burying earlier fine sediment and disturbing OM accumulation and decomposition. This in turn affected metal accumulation and re-distribution in the marginal sediments. Recent anthropogenic markers were found in the deep fine-grained layers, pointing to trace metal migration through the sandy top

layers and subsequent sequestration within the lower clayey and organic-rich layers. These unique marginal profiles are inconsistent with both increasing pollution record at the top of typical modern sedimentary profiles and those displayed by the sediment from the center of the pond (DR5). Thus, the case of Dora Pond demonstrates that human development and land cover change may not only disturb the surface and enhance erosion but can also affect pollution pathways in the environment.

References

Appleby PG, Oldfield F (1978) The calculation of ^{210}Pb dates assuming a constant rate of supply of unsupported ^{210}Pb to the sediment. Catena 5:1–8

Asaf L, Nativ R, Shain D, Hassan M, Geyer S (2004) Controls on the chemical and isotopic compositions of urban stormwater in a semi-arid zone. J Hydrol 294:270–293

Balasoiu CF, Zagury GJ, Deschenes L (2001) Partitioning and speciation of chromium, copper and arsenic in CCA-contaminated soils: influence of soil composition. Sci Total Environ 280:239–255

Biester H, Hermanns YM, Cortizas AM (2012) The influence of organic matter decay on the distribution of major and trace elements in ombrotrophic mires—a case study from the harz mountains. Geochim Cosmochim Acta 84:126–136

Blais JM, Kalff J (1995) The influence of lake morphometry on sediment focusing. Limnol Oceanogr 40:582–588

Bookman R, Driscoll CT, Engstrom DR, Effler SW (2008) Local to regional emission sources affecting mercury fluxes to New York lakes. Atmos Environ 42:6088–6097

Ciszewski D, Czajka A, Bła S (2008) Rapid migration of heavy metals and ^{137}Cs in alluvial sediments. Upper Odra River valley, Poland Environ Geol 55:1577–1586

Clark L (2012) Idrisi GIS and image processing software. Clark University, Worcester

Dan T (1982) Netanya soils and its surroundings. In: Shmueli A, Weber (eds) The book of Netanya, Israel, pp 37–44 (In Hebrew)

Dan Y, Yaalon D (1990) Soil formation in the Sharon and their correspondence to landscape features In: Degani A, Grossman D (eds) HaSharon, Bein Yarkan LaKarmel, Misrad HaBithachon, HaHotsa'a La'Or, Tel-Aviv, Israel, pp 83–97 (In Hebrew)

De Stigter HC, Jesus CC, Boer W, Richter TO, Costa A, van Weering TCE (2011) Recent sediment transport and deposition in the Lisbon–Setúbal and Cascais submarine canyons, Portuguese continental margin. Deep Sea Res Part II Top Stud Oceanogr 58:2321–2344

Dean W (1974) Determination of carbonate and organic matter in calcareous sediments and sedimentary rocks by loss on ignition: comparison with other methods. J Sediment Res 44:242–248

Díaz-Somoano M, Kylander ME, López-Antón MA, Suárez-Ruiz I, Martínez-Tarazona MR, Ferrat M, Kober B, Weiss DJ (2009) Stable lead isotope compositions in selected coals from around the world and implications for present day aerosol source tracing. Environ Sci Technol 43:1078–1085

Du Laing G, Rinklebe J, Vandecasteele B, Meers E, Tack FMG (2009) Trace metal behaviour in estuarine and riverine floodplain soils and sediments: a review. Sci Total Environ 407:3972–3985

Ehrlich S, Karpas Z, Ben-Dor L, Halicz L (2001) High precision lead isotope ratio measurements by multicollector-ICP-MS in variable matrices. J Anal At Spectrom 16:975–977

Ehrlich S, Ben-Dor L, Halicz L (2004) Precise isotope ratio measurement by multicollector-ICP-MS without matrix separation. Can J Anal Sci Spectrosc 49:136–147

Engelmann A, Neber A, Frechen M, Boenigk W, Ronen A (2001) Luminescence chronology of upper Pleistocene and Holocene aeolianites from Netanya South—Sharon coastal plain, Israel. Quaternary Sci Rev 20:799–804

Erel Y, Veron A, Halicz L (1997) Tracing the transport of anthropogenic lead in the atmosphere and in soils using isotopic ratios. Geochim Cosmochim Acta 61:4495–4505

Erel Y, Dayan U, Rabi R, Rudich Y, Stein M (2006) Transboundary transport of pollutants by atmospheric mineral dust. Environ Sci Technol 40:2996–3005

Erel Y, Kalderon-Asael B, Dayan U, Sandler A (2007) European atmospheric pollution imported by cooler air masses to the Eastern Mediterranean during the summer. Environ Sci Technol 41:5198–5203

Farkas A, Erratico C, Vigano L (2007) Assessment of the environmental significance of heavy metal pollution in surficial sediments of the River Po. Chemosphere 68:761–768

Fonseca B, Figueiredo H, Rodrigues J, Queiroz A, Tavares T (2011) Mobility of Cr, Pb, Cd, Cu and Zn in a loamy sand soil: a comparative study. Geoderma 164:232–237

Gonzalez-Fernandez O, Jurado-Roldan AM, Queralt I (2011) Geochemical and mineralogical features of overbank and stream sediments of the Beal Wadi (Cartagena-La Union Mining District, SE Spain): relation to former lead–zinc mining activities and its environmental risk. Water Air Soil Pollut 215:55–65

Guevara SR, Rizzo A, Sánchez R, Arribére M (2003) ^{210}Pb fluxes in sediment layers sampled from Northern Patagonia lakes. J Radioanal Nucl Chem 258:583–595

Gvirtzman G, Wieder M (2001) Climate of the last 53,000 years in the eastern Mediterranean, based on soil-sequence stratigraphy in the coastal plain of Israel. Quat Sci Rev 20:1827–1849

Han FX, Banin A, Kingery WL, Triplett GB, Zhou LX, Zheng SJ, Ding WX (2003) New approach to studies of heavy metal redistribution in soil. Adv Environ Res 8:113–120

Harlavan Y, Almogi-Labin A, Herut B (2010) Tracing natural and anthropogenic Pb in sediments along the Mediterranean coast of Israel using Pb isotopes. Environ Sci Technol 44:6576–6582

He Q, Walling DE (1996) Interpreting particle size effects in the adsorption of ^{137}Cs and unsupported ^{210}Pb by mineral soils and sediments. J Environ Radioact 30:117–137

Heim S, Schwarzbauer J (2013) Pollution history revealed by sedimentary records: a review. Environ Chem Lett 11:255–270

Kirchner G (2011) ^{210}Pb as a tool for establishing sediment chronologies: examples of potentials and limitations of conventional dating models. J Environ Radioactiv 102:490–494

Koyumdjisky H, Dan Y, Suriano S, Nisim S (1988) Selected soil sections from Israel soils. In: Beit Dagan: Volcani center, Pedology Department, Israel pp.131–132 (In Hebrew)

Levin N, Kidron GJ, Ben-Dor E (2007) Surface properties of stabilizing coastal dunes: combining spectral and field analyses. Sedimentology 54:771–788

Levin N, Elron E, Gasith A (2009) Decline of wetland ecosystems in the coastal plain of Israel during the 20th century: implications for wetland conservation and management. Landscape Urban Plan 92:220–232

Levy I, Levin N, Yuval SJD, Kark JD (2015) Back-extrapolating a land use regression model for estimating past exposures to traffic-related air pollution. Environ Sci Technol 49:3603–3610

Martin MH, Coughtrey PJ (1982) Biological monitoring of heavy metals pollution. In: Mellanby K (ed). Applied Science. London, UK pp. 253–271

Nriagu JO (1996) A history of global metal pollution. Science 272:223–224

Pacyna JM, Pacyna EG (2001) An assessment of global and regional emissions of trace metals to the atmosphere from anthropogenic sources worldwide. Environ Rev 9:269–298

Platzner I, Ehrlich S, Halicz L (2001) Isotope-ratio measurements of lead in NIST standard reference materials by multiple-collector inductively coupled plasma mass spectrometry. J Anal Chem 370:624–628

Rauch JN, Pacyna JM (2009) Earth's global Ag, Al, Cr, Cu, Fe, Ni, Pb, and Zn cycles. Global Biogeochem Cycles 23

Richards BK, Steenhuis TS, Peverly JH, McBridge MB (1998) Metal mobility at an old, heavily-loaded sludge application site. Environ Pollut 99:365–377

Richards BK, Steenhuis TS, Peverly JH, McBridge MB (2000) Effects of sludge-processing mode, soil texture and soil pH on metal mobility in undisturbed soil columns under accelerated loading. Environ Pollut 109:327–346

Rieuwert JS, Thornton I, Farago ME, Ashmore MR (1998) Factors influencing metal bioavailability in soils: preliminary investigations for the development of a critical loads approach for metals. Chem Spec Bioavailab 10:61–75

Slowik M, Sobczyn T, Młynarczyk Z (2010) Types of sedimentary environment in alluvial sediments distinguished on the basis of its chemical constitution: the example of the lower course of the Obra River (Western Poland). Environ Earth Sci 59:957–966

Tang Z, Engel BA, Pijanowski BC, Lim KJ (2005) Forecasting land use change and its environmental impact at a watershed scale. J Environ Manag 76:35–45

Temminghoff EJM, Van der Zee SEATM, DeHaan FAM (1997) Copper mobility in a copper-contaminated sandy soil as affected by pH and solid and dissolved organic matter. Environ Sci Technol 31:1109–1115

Teutsch N (1999) Distribution and mobility of lead in the soil: isotopic composition as an indicator for natural versus anthropogenic sources. PhD thesis. The Hebrew University in Jerusalem

Teutsch N, Erel Y, Halicz L, Banin A (2001) Distribution of natural and anthropogenic lead in Mediterranean soils. Geochim Cosmochim Acta 65:2853–2864

Tiefenthaler LL, Stein ED, Schiff KC (2008) Watershed and land use-based sources of trace metals in urban storm water. Environ Toxicol Chem 27:277–287

Townsend AT, Seen AJ (2012) Historical lead isotope record of a sediment core from the Derwent River (Tasmania, Australia): a multiple source environment. Sci Total Environ 424:153–161

Tsoar H (1990) The ecological background, deterioration and reclamation of desert dune sand. Agric Ecosyst Environ 33:147–170

Vane CH, Chenery SR, Harrison I, Kim AW, Moss-Hayes V, Jones DG (2011) Chemical signatures of the Anthropocene in the Clyde estuary, UK: sediment-hosted Pb, $^{207/206}$Pb, total petroleum hydrocarbon, polyaromatic hydrocarbon and polychlorinated biphenyl pollution records. Phil Trans R Soc A 369:1085–1111

Walraven N, van Os BJH, Klaver GT, Middleburg JJ, Davis GR (2014) Reconstruction of historical atmospheric Pb using Dutch urban lake sediments: a Pb isotope study. Sci Total Environ 484:185–195

Weiss D, Shotyk W, Appleby PG, Kramers JD, Cheburkin AK (1999) Atmospheric Pb deposition since the industrial revolution recorded by five Swiss peat profiles: enrichment factors, fluxes, isotopic composition, and sources. Environ Sci Technol 33:1340–1352

Wong CS, Li X, Thornton I (2006) Urban environmental geochemistry of trace metals. Environ Pollut 142:1–16

Yaalon DH, Ganor E (1973) The influence of dust on soils during the Quaternary. Soil Sci 116:146–155

Yair A (1990) Runoff generation in a sandy area—the Nizzana sands, Western Negev, Israel. Earth Surf Proc Land 15:597–609

Yair A, Kossovsky A (2002) Climate and surface properties: hydrological response of small arid and semi-arid watersheds. Geomorphology 42:43–57

Yair A, Raz-Yassif N (2004) Hydrological processes in a small arid catchment: scale effects of rainfall and slope length. Geomorphology 61:155–169

Zohar I, Bookman R, Levin N, de Stigter H, Teutsch N (2014) Contamination history of lead and other trace metals reconstructed from an urban winter pond in the eastern Mediterranean Coast (Israel). Environ Sci Technol 48:13592–13600